Applied Physics Letters

Interface carbon defects at 4H-SiC(0001)/ SiO_2 interfaces studied by electron-spin-resonance spectroscopy

Cite as: Appl. Phys. Lett. **113**, 061605 (2018); https://doi.org/10.1063/1.5041059
Submitted: 23 May 2018 . Accepted: 26 July 2018 . Published Online: 09 August 2018

T. Umeda, G.-W. Kim, T. Okuda, M. Sometani, T. Kimoto, and S. Harada

Interface carbon defects at 4H-SiC(0001)/SiO_2 interfaces studied by electron-spin-resonance spectroscopy

T. Umeda,[1,a)] G.-W. Kim,[1] T. Okuda,[2] M. Sometani,[3] T. Kimoto,[2] and S. Harada[3]
[1]*Institute of Applied Physics, University of Tsukuba, Tsukuba 305-8573, Japan*
[2]*Graduate School of Engineering, Kyoto University, Kyoto 615-8510, Japan*
[3]*National Institute of Advanced Industrial Science and Technology (AIST), Tsukuba 305-8569, Japan*

(Received 23 May 2018; accepted 26 July 2018; published online 9 August 2018)

We study an electron-spin-resonance (ESR) signal of carbon dangling-bond defects at 4H-SiC(0001)/SiO_2 interfaces, which we call an "interface carbon defect." The ESR signal is close to a *c*-axial type of the P_{bC} centers (interfacial carbon dangling bonds) that have originally been found in porous-SiC/SiO_2 interfaces. The interface carbon defects were always formed with an areal density of $3–4 \times 10^{12}\,cm^{-2}$ after the standard dry oxidation of 4H-SiC(0001) surfaces. They act as electron traps and decrease the amount of free electrons in the channel region, consequently reducing the field-effect mobility of Si-face 4H-SiC MOSFETs. They were eliminated by optimum post-oxidation anneals (POAs) in either NO or $POCl_3$ environment. Furthermore, $POCl_3$ POAs at 1000 °C introduced a high density ($1.7 \times 10^{12}\,cm^{-2}$) of phosphorus donors into the channel region, increasing the free-carrier density as compared with the case of NO POAs. *Published by AIP Publishing.*
https://doi.org/10.1063/1.5041059

The 4H-SiC/SiO_2 interfaces are the key components for SiC power devices such as 4H-SiC metal-oxide-semiconductor field-effect transistors (MOSFETs). The current standard technique for fabricating a good 4H-SiC/SiO_2 interface is a high-temperature (1200–1300 °C) thermal oxidation of a 4H-SiC(0001) surface (the so-called "Si face") by dry O_2 gas followed by a post-oxidation anneal (POA) in a NO environment. The POA process can make the field-effect mobility (μ_{FE}) of 4H-SiC MOSFETs ten times larger than that before the POA.[1,2] The mechanism for this drastic μ_{FE}-improvement has recently been clarified by combining Hall and split capacitance-voltage measurements.[3] According to the recent findings, the NO POA process effectively increases the amount of free electrons by removing electron traps, while it does not increase the electron mobility itself much. The amount of the removed traps was found to be $2–3 \times 10^{12}\,cm^{-2}$ for the standard NO POA recipe.[3] However, the origin of such electron traps associated with the μ_{FE}-degradation is still unclear. So far, electron-spin-resonance (ESR) spectroscopy, which is a powerful tool for identifying microscopic origins of defect levels, has been applied to SiC-MOS systems.[4–6] Up to now, however, ESR centers with $2–3 \times 10^{12}\,cm^{-2}$ or more have not been detected at the 4H-SiC(0001)/SiO_2 interfaces. Alternatively, electrically detected magnetic resonance (EDMR) was applied to Si-face 4H-SiC MOSFETs to visualize interface defects in their MOS interfaces.[7–10] As a result, an interfacial Si-vacancy center[8] and different types of interface defects[7,9,10] have been detected under optimum bias conditions for each EDMR signal. However, the densities of these EDMR centers are unclear yet because of a lack of quantitativity of EDMR signals.

In this Letter, we present quantitative ESR measurements on interface defects or electron traps at 4H-SiC(0001)/SiO_2 interfaces formed by dry oxidation with/without the standard NO POA process. Furthermore, we also characterized another effective POA process, i.e., $POCl_3$ POA,[11,12] which is known to achieve a much higher μ_{FE} ($\sim$100 cm^2/V s) than the standard NO POA (20–40 cm^2/V s).[11] By applying ESR to special free-standing 4H-SiC epitaxial layers, we observed an anisotropic ESR signal just after the dry oxidation. This signal is assigned to be a sort of a carbon dangling-bond center at the 4H-SiC(0001)/SiO_2 interfaces, since it resembles *c*-axial type P_{bC} centers (carbon dangling bonds) that have originally been found in porous-SiC/SiO_2 interfaces.[6] We here call it an "interface carbon defect." Our ESR measurements demonstrated that both optimum NO and $POCl_3$ POAs can remove it. Their spin density was estimated to be $3–4 \times 10^{12}\,cm^{-2}$, which is in agreement with the amount of electron traps changed by NO POAs.[3] Thus, we conclude that the interface carbon defects are major electron traps that decrease the μ_{FE} of dry-oxidized Si-face MOSFETs. In addition, we also found phosphorus (P) doping over $1 \times 10^{12}\,cm^{-2}$ after an optimum $POCl_3$ POA process, which contributes to an increase in the free-carrier density in the channel region. In contrast, we could not detect nitrogen (N) doping after NO POAs, and hence evaluated the N-doping density to be lower than $1 \times 10^{11}\,cm^{-2}$.

We carried out ESR measurements on the interface carbon defects at room temperature and on the P and N donors at 4–20 K by means of a Bruker E500 X-band spectrometer equipped with a super-high-Q cavity and an Oxford ESR-900 liquid-He cryostat. Since the carbon interface defect showed a strong microwave saturation behavior due to a weak spin-orbit interaction of its electron spin on a carbon atom, its ESR signal was most clearly observable at room temperature. We utilized the standard magnetic-field modulation technique at 100 kHz with an amplitude of 0.1–0.3 mT for the interface carbon defect. ESR transitions were excited by a microwave of 9.428 GHz and 0.2 mW, unless otherwise

[a)]Author to whom correspondence should be addressed: umeda@bk.tsukuba.ac.jp

stated. The spin densities were calculated by comparing their absorption ESR intensity per cm^2 with that of a measurement standard (a $CuSO_4 \cdot 5H_2O$ specimen with 12.53 mg and 3.02×10^{19} spins).

The ESR substrates were prepared using free-standing 4H-SiC epitaxial layers ($0.35 \times 0.70 \times 0.013\,cm^3$ or $0.35 \times 0.70 \times 0.016\,cm^3$) with either Al doping of $4 \times 10^{14}\,cm^{-3}$ or N doping of $4 \times 10^{14}\,cm^{-3}$, respectively. In these epitaxially grown crystals, the amount of deep levels is controlled to be much lower than the above doping levels, and hence an obstruction due to bulk ESR signals should be suppressed to be $10^{11}\,cm^{-2}$ ($=10^{13}\,cm^{-3} \times 0.01$ cm) or lower. This is the key for observing interface ESR signals with a density of $10^{12}\,cm^{-2}$.

Both sides of the substrates were finished by chemical mechanical polishing (CMP); however, the substrates showed a broad amorphous-carbon signal [g value (g) = 2.003, Fig. 1(a)], in addition to a reference signal of the E' center (a paramagnetic silicon center in SiO_2,[13] $g = 2.0008$) in a sample rod. The amorphous-carbon signal is consistent with those of carbon dangling bonds in various carbon materials.[14–16] The signal is isotropic, as indicated by solid and dotted lines in Fig. 1(a) measured for different magnetic-field angles. The isotropy was also confirmed by a more detailed angular dependence shown in Fig. 2(a). The peak-to-peak signal width (0.55 mT) is consistent with those of sp^3-hybridizied carbons.[15] We attribute the signal's origin to be residual carbons on the polished surfaces, because its ESR intensities strongly depended on CMP processes as well as on the surface etching detailed below. Note that this signal could not have been removed by either RCA chemical cleaning or sacrificed oxidation (50 nm) + SiO_2 wet etching; so, we have to use a different surface treatment. To eliminate the amorphous-carbon signal, we carried out a precise dry-etch process by a high-temperature HCl anneal (Table I).[17] We hereafter call this the "reset process." After the reset process, the amorphous-carbon signal was completely eliminated as shown in Fig. 1(b). The reset process was also very useful for preparing a fresh surface of the substrate by removing its on-top SiO_2 layer as well as the surface layer of the substrate.

By taking advantage of the reset process, we could repeatedly characterize dry oxidation and various POA processes (see Table I) on the fresh surfaces, as demonstrated in Figs. 1(c)–1(h). It is notable that the oxidation and POA processes we studied here were electrically characterized by previous works on MOS or MOSFET structures.[2,3,9,12] In the first step, we repeatedly tried dry oxidation. For ESR specimens after the dry oxidation, their Si face was protected by an acid-proof coat, and then C-face oxide was chemically removed by hydrofluoric-acid etching. This process ensures that we measured only ESR-active centers on the side of the Si face, and the C-face side will be separately studied elsewhere. We always observed the appearance of a spin-1/2 ESR signal, which we call an "interface carbon defect," as seen in Figs. 1(c), 1(e), and 1(g). As is shown by solid and dotted lines in Fig. 1(c), this signal is clearly anisotropic,

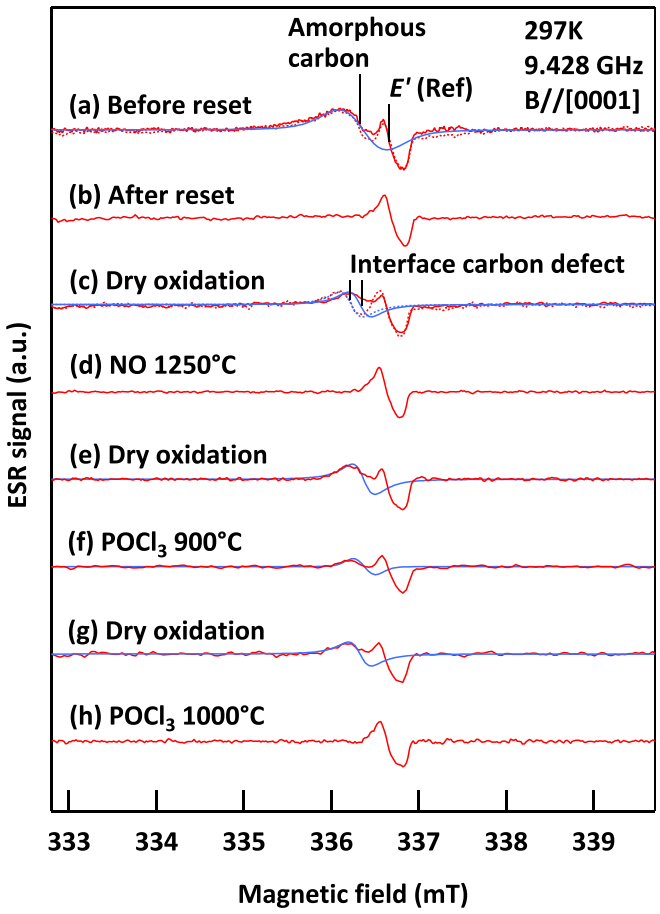

FIG. 1. Room-temperature ESR spectra of free-standing 4H-SiC(0001) epitaxial layers before/after oxidation and post-oxidation anneals (POAs), where an E' reference signal comes from a sample rod. Solid and dotted lines were measured for magnetic fields (**B**) parallel and normal to the [0001] axis, respectively (cf., Fig. 2). (a) Initial substrate. (b) After the reset process. (c), (e), and (g) After the standard dry oxidation on the Si face of the reset substrate. An anisotropic ESR signal of "interface carbon defect" appears. (d), (f), and (h) After POAs with either NO or $POCl_3$.

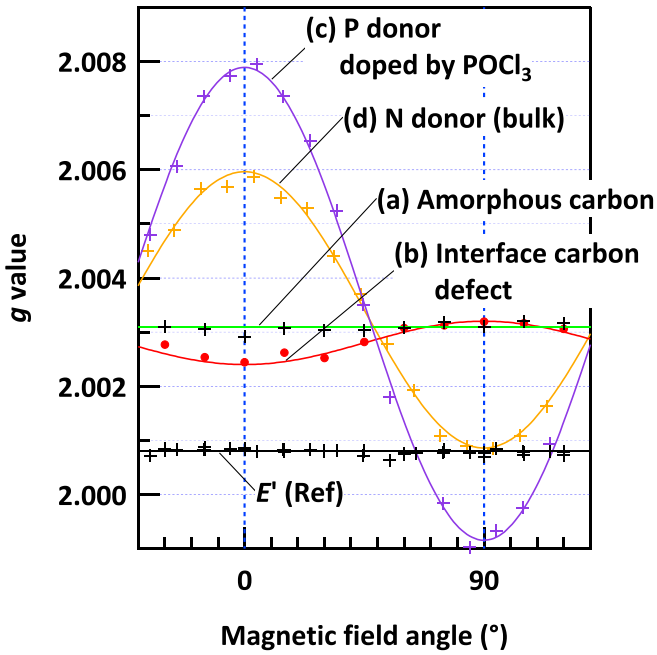

FIG. 2. Angular dependence of ESR signals observed in this study. Magnetic-field angles of 0° and 90° correspond to magnetic fields parallel and normal to the [0001] axis, respectively. (a) Amorphous-carbon signal in initial substrates. (b) Interface carbon defect formed at dry-oxidized 4H-SiC(0001)/SiO_2 interfaces. (c) Phosphorus donors (measured at 4 K) doped after $POCl_3$ POA at 1000 °C. (d) Nitrogen donors (measured at 20 K) originating from residual impurities in bulk.

TABLE I. Oxidation and optimum POA processes on 4H-SiC(0001) (Si face) examined in this study. The reset process as well as ESR results are also summarized.

Process	Condition	ESR result
Reset	HCl anneal at 1300 °C for 2 min. (etching rate for SiC = 14 nm/2 min.)	Remove surface amorphous-carbon signal
Dry oxidation	O_2 anneal at 1300 °C for 30 min. (44-nm-thick SiO_2 growth on Si face)	Generate interface carbon defects with 3–4 × 10^{12} cm^{-2}
NO POA	NO anneal at 1250 °C for 70 min. followed by N_2 anneal at 1200 °C for 30 min.	Remove interface carbon defects
$POCl_3$ POA	$POCl_3$ anneal at 1000 °C for 10 min. followed by N_2 anneal at 1000 °C for 30 min.	Remove interface carbon defects + P-doping

unlike the amorphous-carbon signal noted above as well as the interfacial Si-vacancy signal studied by Cochrane *et al.*[8] By examining its angular dependence in detail [Fig. 2(b)], we found that this signal shows *c*-axial symmetry with $g_{//} = 2.0024$ and $g_{\perp} = 2.0032$. These principal g values belong to those of typical carbon dangling bonds.[14] It is especially worth noting that the principal g values show excellent agreement with those of the *c*-axial P_{bC} center ($g_{//} = 2.0023$ and $g_{\perp} = 2.0032$), which has been identified as *c*-axial carbon dangling bonds in porous-SiC/SiO_2 interfaces.[6] Therefore, the interface carbon defect most probably originates from a sort of carbon dangling bonds at the 4H-SiC(0001)/SiO_2 interfaces. However, the final identification of this defect should wait until its hyperfine interactions with a ^{13}C nuclear spin have been fully analyzed.

In the second step, we examined the changes in the interface carbon defects by subjecting the dry-oxidized substrates to either NO or $POCl_3$ POA processes. As Fig. 1(d) shows, the interface carbon defects were eliminated by an optimum NO POA (Table I). Their amount was reduced below our detection limit. Also, an optimum $POCl_3$ POA process (Table I) achieved the same result, as shown in Fig. 1(h). On the other hand, for $POCl_3$ POA at a slightly lower temperature (900 °C), the interface carbon defects could not be fully removed [Fig. 1(f)]. This observation is consistent with the previous experimental finding that the carrier traps were effectively annihilated by $POCl_3$ anneal at over 950 °C.[12]

For each process step, the spin densities of the carbon defects (amorphous carbon or interface carbon defect) were estimated by deconvoluting a carbon-defect signal from each spectrum (blue lines in Fig. 1). The quantitative values are summarized in Fig. 3. As shown in Fig. 3(a), we found the amorphous-carbon signal with 4.9 × 10^{12} cm^{-2}/one-side (we assumed this signal from both faces of a substrate). In other substrates with different CMP processes, its spin density decreased below 1 × 10^{12} cm^{-2}. After the reset process, no substrates showed the amorphous-carbon signal, e.g., shown in Fig. 3(b).

After the dry oxidation processes, we always found the interface carbon defects with 3–4 × 10^{12} cm^{-2} [Figs. 3(c), 3(e), and 3(g)]. They could be fully eliminated by the optimum NO and $POCl_3$ POA processes as shown in Figs. 3(d) and 3(h), respectively. In the previous work,[3] a NO POA process (1250 °C for 60 min. applied to a 50-nm-thick dry oxide) reduced the amount of electron traps at the interface by 2–3 × 10^{12} cm^{-2}, resulting in significantly improving μ_{FE}. Such a reduction is mostly consistent with the present result that the interface carbon defects with 3–4 × 10^{12} cm^{-2} are eliminated by a NO POA process. Furthermore, the interface carbon defect expectedly works as an electron trap, because its positive and neutral dangling-bond levels can capture electron(s), the same as in the case of famous P_b centers (silicon dangling bonds) at Si/SiO_2 interfaces.[13] We therefore propose that the observed defects are responsible for causing the electron traps associated with the μ_{FE}-variation before/after NO POAs.

Interestingly, the $POCl_3$ anneal can further increase μ_{FE} up to 100 cm^2/V s.[11] The present result revealed that both the optimum $POCl_3$ and NO POAs fully remove the interface carbon defects. The additional increment in μ_{FE} after the $POCl_3$ anneal is possibly due to the P-doping with the channel region. Figure 4 shows the P-doping after the optimum $POCl_3$ anneal. In the figure, ESR spectra measured at 4 K by a rapid-passage mode,[18] which exhibit absorption ESR signals, were examined for (a) the reset surface, (b) and (c) $POCl_3$ POAs at different temperatures, and (d) NO POA. In Fig. 4(c), a new broad resonance appears, which we attribute to the P-donor signal. A doublet hyperfine (HF) splitting of a ^{31}P nucleus (nuclear spin = 1/2, natural abundance = 100%) seems to be obscured by a broad signal width which is comparable to the ^{31}P HF splitting (0.29 mT) of bulk P donors,[19] as shown in Fig. 4(c). Moreover, we speculate that the ^{31}P HF splitting itself may be shrinked rather than that of the bulk donors. In fact, the g principal values of the present P donors are determined to be $g_{//} = 2.0079$ and $g_{\perp} = 1.9992$ [see Fig. 2(c)], which deviate from those of the bulk P donors in 4H-SiC

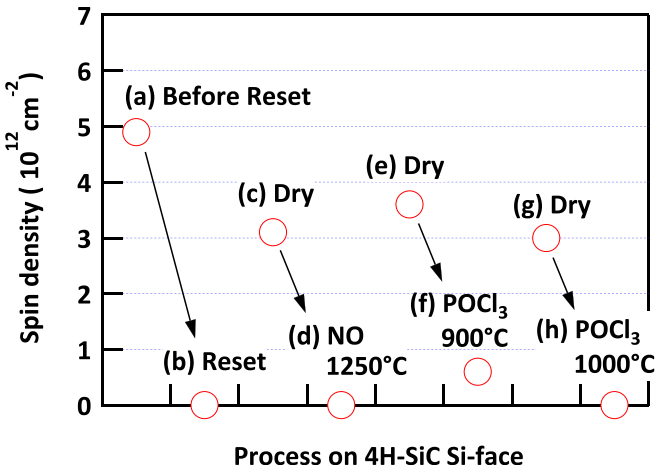

FIG. 3. Spin densities of carbon defects measured for ESR spectra (a) to (h) in Fig. 1. (a) Amorphous-carbon defect of an initial substrate. We assume that this signal arises from both Si- and C-faces of the substrate. (b) After the reset process. The reset process was also used to initialize the substrate after (d), (f), and (h). (c), (e), and (g) Interface carbon defect formed at dry-oxidized 4H-SiC(0001)/SiO_2 interfaces. (d) After an optimum NO POA following to (c). (f) and (h) After $POCl_3$ POAs at different temperatures.

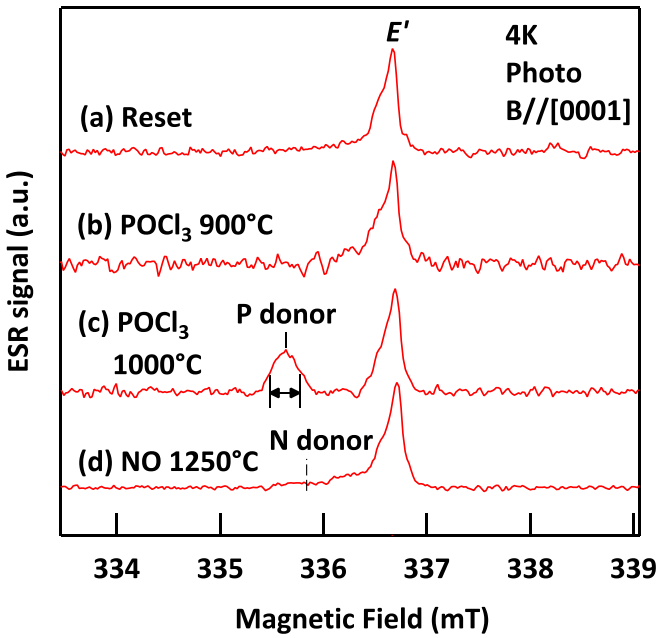

FIG. 4. Phosphorus doping after $POCl_3$ POAs. ESR spectra were measured using a rapid-passage technique (out-of-phase and second-harmonic detections with 2-mW microwave excitation) at 4 K under photo illumination (100-W halogen lamp), which show absorption ESR signals of P and N donors. (a) Initial substrate. (b) and (c) After $POCl_3$ POAs. An arrow indicates a doublet ^{31}P hyperfine splitting (0.29 mT) of the bulk P donor.[19] (d) After NO POA.

($g_{//} = 2.0065$ and $g_{\perp} = 2.0006$).[19] This deviation may reflect the fact that the present P donors are located close to the interface, possibly perturbing their donor states. Actually, an interface-induced perturbation was theoretically predicted for conduction-band-edge states.[20]

The signal intensity of the P donors is in proportion to their spin density; however, a rapid-passage signal intensity cannot be straightforwardly compared with the signal intensity of $CuSO_4{\cdot}5H_2O$. Therefore, for a comparison, we employed a rapid-passage signal of the EI6 center in a different sample (bulk carbon vacancies,[21] $8.3 \times 10^{12}\,cm^{-2}$) observed at 4 K with the same microwave power (2 mW). Since this center resembles the present P donor in terms of their microwave-saturation behaviors, we could directly compare their rapid-passage signals. Using such a standard, we estimated the P-doping density to be $1.7 \times 10^{12}\,cm^{-2}$. If we assume a uniform doping thickness of 5 nm, the P-doping density becomes $3 \times 10^{18}\,cm^{-3}$, which is close to the observed carrier density of $4 \times 10^{18}\,cm^{-3}$ at a $POCl_3$-annealed 4H-SiC(0001)/SiO_2 interface measured by a scanning capacitance microscope (SCM).[22] Note that the P-doping density is comparable to the density of the interface carbon defects. The P-doping is therefore expected to increase the free-carrier density in the channel region as comparable as the case of the interface carbon defects. On the other hand, the ionized P donors simultaneously increase carrier scattering, consequently deteriorating the carrier mobility. Even including such deterioration, the increase in the free-carrier density due to P-doping may realize the higher μ_{FE} after $POCl_3$ POAs, because the lack of mobile carriers strongly limited μ_{FE} even after POAs.[3] It is also confirmed that the P donors were completely removed after the reset process, indicating that they are introduced into a very shallow region within 14 nm from the interface.

On the contrary, the P-doping was not observed at 900 °C [Fig. 4(b)], and the elimination of the interface carbon defects was not perfect [Fig. 3(f)]. The reason why P-doping was observable at 1000 °C is ascribed to strong re-oxidation during the POAs at 1000 °C.[12] It is reasonable to consider that such a strong re-oxidation enables the mixing of P atoms and the SiC lattice, enhancing the substitutional doping of P atoms into SiC. According to the carrier-lifetime measurement,[12] the $POCl_3$ POAs effectively increased the carrier lifetimes in both *n*- and *p*-type 4H-SiC epi-layers. The present result also accounts for such behaviors because a neutral dangling-bond center can capture both an electron and a hole, which is known in the case of the P_b center.[13]

In contrast, for the NO POAs [Fig. 4(d)], we could not find any increment in the N-donor signal, although the bulk N donors were clearly observable at 20 K and their angular dependence could be traced as shown in Fig. 2(d). Accordingly, we judged that the N-doping density should be at least one order of magnitude lower ($<1 \times 10^{11}\,cm^{-2}$ or $<2 \times 10^{17}\,cm^{-3}$ when we assume a uniform N-doping layer of 5 nm in thickness) than the P-doping density observed in Fig. 4(c). At least, for the NO POAs, the elimination of the carbon interface defects should have a much larger impact on μ_{FE} than the N-doping effect. The present result seems to be consistent with those in the previous SCM study that reported the carrier density of $5 \times 10^{17}\,cm^{-3}$ at a NO-annealed interface.[22]

In summary, we have presented quantitative ESR analyses on "interface carbon defects" with 3–4 $\times 10^{12}\,cm^{-2}$ that were assigned to a sort of carbon dangling bonds at 4H-SiC(0001)/SiO_2 interfaces, closely resembling *c*-axial type P_{bC} centers.[6] They could be fully eliminated by optimum POAs by NO or $POCl_3$. Based on the similarities between our ESR data and previous electrical characterization,[2,3,9,12] we suggest that the interface carbon defects are the major electron traps at the dry-oxidized 4H-SiC(0001)/SiO_2 interfaces, and hence both the POAs drastically improve μ_{FE} of Si-face 4H-SiC MOSFETs. In addition, we found that the $POCl_3$ POAs at 1000 °C formed a high density ($>1 \times 10^{12}\,cm^{-2}$) of the P donors in the channel region, which is possibly related to further enhancement on μ_{FE}. In contrast, the N-doping effect has a much smaller impact on μ_{FE} than the elimination of the interface carbon defects.

This work was supported by the Council for Science, Technology and Innovation (CSTI), Cross-ministerial Strategic Innovation Promotion Program (SIP), and "Next-generation power electronics" (funding agency: NEDO). This work was also partly supported by a Grant-in-Aid (Grant No. 17H02781) from the Ministry of Education, Culture, Sports, Science and Technology of Japan.

[1]G. Y. Chung, C. C. Tin, J. R. Williams, K. McDonald, R. K. Chanana, R. A. Weller, M. Di Ventra, S. T. Pantelides, L. C. Feldman, O. W. Holland, M. K. Das, and J. W. Palmour, IEEE Electron Device Lett. **22**, 176 (2001).
[2]H. Yoshioka, J. Senzaki, A. Shimozato, Y. Tanaka, and H. Okumura, AIP Adv. **5**, 017109 (2015).

[3]T. Hatakeyama, Y. Kiuchi, M. Sometani, S. Harada, D. Okamoto, H. Yano, Y. Yonezawa, and H. Okumura, Appl. Phys. Express **10**, 046601 (2017).
[4]V. V. Afanas'ev, F. Ciobanu, S. Dimitrijev, G. Pensl, and A. Stesmans, Mater. Sci. Forum **483–485**, 563 (2005).
[5]P. J. MacFarlane and M. E. Zvanut, J. Appl. Phys. **88**, 4122 (2000).
[6]J. L. Cantin, H. J. von Bardeleben, Y. Shishkin, Y. Ke, R. P. Devaty, and W. J. Choyke, Phys. Rev. Lett. **92**, 015502 (2004).
[7]D. J. Meyer, P. M. Lenahan, and A. J. Lelis, Appl. Phys. Lett. **86**, 023503 (2005).
[8]C. J. Cochrane, P. M. Lenahan, and A. J. Lelis, J. Appl. Phys. **109**, 014506 (2011).
[9]T. Umeda, M. Okamoto, R. Kosugi, R. Arai, Y. Sato, S. Harada, T. Makino, and T. Ohshima, ECS Trans. **58**, 55 (2013).
[10]G. Gruber, J. Cottom, R. Meszaros, M. Koch, G. Pobegen, T. Aichinger, D. Peters, and P. Hadley, J. Appl. Phys. **123**, 161514 (2018).
[11]D. Okamoto, H. Yano, T. Hatayama, and T. Fuyuki, Appl. Phys. Lett. **96**, 203508 (2010).
[12]T. Okuda, T. Kobayashi, T. Kimoto, and J. Suda, Appl. Phys. Express **9**, 051301 (2016).
[13]P. M. Lenahan and J. F. Conley, Jr., J. Vac. Sci. Technol. B **16**, 2134 (1998); P. M. Lenahan and P. V. Dressendorfer, J. Appl. Phys. **54**, 1457 (1983).
[14]J. Robertson, Mater. Sci. Eng. R **37**, 129 (2002).
[15]A. Bateni, E. Erdem, S. Repp, S. Acar, I. Kokal, W. Häßler, S. Weber, and M. Somer, J. Appl. Phys. **117**, 153905 (2015).
[16]R. Genc, M. O. Alas, E. Harputlu, S. Repp, N. Kremer, M. Castellano, S. G. Colak, K. Ocakoglu, and E. Erdem, Sci. Rep. **7**, 11222 (2017).
[17]S. Nakamura, T. Kimoto, H. Matsunami, S. Tanaka, N. Teraguchi, and A. Suzuki, Appl. Phys. Lett. **76**, 3412 (2000).
[18]R. S. Alger, *Electron Paramagnetic Resonance: Techniques and Applications* (Interscience Publishers, New York, 1968), pp. 21–25.
[19]N. T. Son, A. Henry, J. Isoya, M. Katagiri, T. Umeda, A. Gali, and E. Janzén, Phys. Rev. B **73**, 075201 (2006).
[20]Y. Matsushita and A. Oshiyama, Nano Lett. **17**, 6458 (2017).
[21]T. Umeda, J. Isoya, N. Morishita, T. Ohshima, T. Kamiya, A. Gali, P. Deák, N. T. Son, and E. Janén, Phys. Rev. B **70**, 235212 (2004).
[22]P. Fiorentza, F. Giannazzo, M. Vivona, A. La Magna, and F. Roccaforte, Appl. Phys. Lett. **103**, 153508 (2013).